View Article Online / Journal Homepage / Table of Contents for this issue

Atomic force microscope studies of fibrinogen adsorption

Laurel E. Averett[a] and Mark H. Schoenfisch*[b]

Received 25th November 2009, Accepted 9th March 2010
First published as an Advance Article on the web 30th March 2010
DOI: 10.1039/b924814e

Published on 30 March 2010. Downloaded by Michigan State University on 19/01/2016 16:46:48.

Since its invention in 1986 by Binnig, Quate, and Gerber, the atomic force microscope (AFM) has proven to be an extremely useful tool for examining the interactions of proteins with surfaces. Fibrinogen in particular has been used as a model protein to demonstrate new methodologies for studying protein behavior with AFM due to its unique size, shape, and function. Indeed, fibrinogen's central role in both blood coagulation and blood-based infections has made it the primary protein used to interrogate the biocompatibility of surfaces. The goal of this review is to provide an analytical perspective on the utility of AFM for investigating the interaction of fibrinogen with surfaces.

1. Introduction

When a foreign object such as a medical device (*e.g.*, catheter) is introduced into the blood stream, our body responds by coating the implant with plasma proteins including fibrinogen that subsequently trigger the coagulation cascade, resulting in platelet adhesion and the formation of a thrombus on the surface.[1] With time the "clot" may block blood flow at the site and/or embolize to cause heart attack or stroke. Equally problematic, protein-coated surfaces serve as a platform to which bacteria adhere, proliferate, and form biofilms. Examining the influence of a surface's physical and chemical properties on fibrinogen adsorption may facilitate the design of more biocompatible interfaces.

Fibrinogen is the soluble precursor to fibrin, the polymerized protein network that serves as the structural scaffold of blood clots.[2] Fibrinogen is a symmetrical 340 kDa plasma protein comprised of three pairs of peptide chains, the Aα, Bβ, and γ (Fig. 1a). The N-termini of all six chains meet in a disulfide-rich region in the center of the molecule termed the E region. The C-termini of the Bβ and γ chains form independently folded globular modules that together comprise two distal D domains. The C-terminus of the Aα chain extends away from the molecule to form a small globular αC domain. One of each of the three pairs of chains participates in the two coiled-coil regions that connect the D and E regions. When observed using a high-resolution microscope (*e.g.*, electron or atomic force), fibrinogen has a trinodular shape representing the D–E–D arrangement of the domains (Fig. 1b).

As a multifunctional tool capable of high-resolution, multi-faceted imaging and force spectroscopy, the atomic force microscope (AFM) has enabled exquisite examination of fibrinogen adsorption to and interaction with surfaces. Briefly, the AFM consists of a small cantilever controlled in the *z*-direction by a piezoelectric crystal.[3] An optical lever is created by a beam of light from a light-emitting diode reflected off of the cantilever onto a position-sensitive photodiode (Fig. 2). Deflections of the cantilever cause changes in the position of the light spot (*i.e.*, changes in the voltage detected by the photodiode). Since the cantilevers are homogeneous and the cantilever deviations

[a]*Department of Physics, University of North Carolina at Chapel Hill, Chapel Hill, NC, 27599, USA*
[b]*Department of Chemistry, University of North Carolina at Chapel Hill, Chapel Hill, NC, 27599, USA. E-mail: schoenfisch@unc.edu*

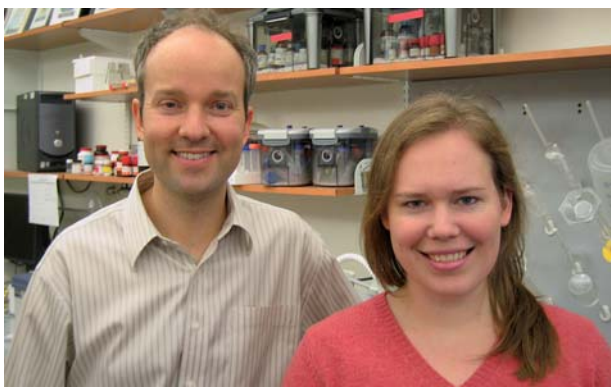

Mark H. Schoenfisch and Laurel E. Averett

Mark Schoenfisch is a Professor of Chemistry in the Department of Chemistry at the University of North Carolina at Chapel Hill (UNC-Chapel Hill). Dr Schoenfisch earned undergraduate degrees in Chemistry (BA) and Germanic Languages and Literature (BA) at the University of Kansas prior to attending the University of Arizona for graduate studies in Chemistry (PhD). Before starting at UNC-Chapel Hill, he spent two years as a National Institutes of Health Postdoctoral Fellow at the University of Michigan. His research interests span biomaterials, chemical sensors, nitric oxide release scaffolds, and scanning probe microscopy.

Laurel Averett earned her PhD in Dr Schoenfisch's lab studying the interactions responsible for fibrin polymerization using atomic force microscopy. She completed an undergraduate degree in Physics at the College of William and Mary (BS) and has earned an MS in Physics with a concentration in Biophysics from UNC-Chapel Hill.

View Article Online

Published on 30 March 2010. Downloaded by Michigan State University on 19/01/2016 16:46:48.

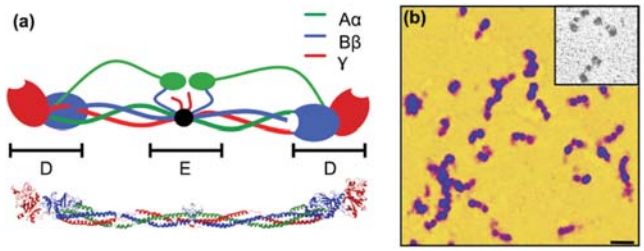

Fig. 1 (a) Crystal structure (bottom) and schematic (top) of fibrinogen molecule. The N-termini of the Aα and Bβ chains and the αC domains are not shown in the crystal structure. Protein Data Bank entry 3GHG was used to make the crystal structure. (b) AFM and transmission electron microscope (inset) images of single fibrinogen molecules on mica substrates. Note the trinodular morphology of each molecule, representing the D–E–D region structure of fibrinogen. The αC domains of some molecules are discerned winding away from the bulk of the molecule. While electron microscopy images can often resolve the differences in size between the E and D domains, AFM images typically cannot. AFM image reprinted with permission from Abou-Saleh *et al.*[26] Copyright 2009, Elsevier, transmission electron microscope image reprinted with permission from Veklich *et al.*[83] Copyright 1993, The American Society for Biochemistry and Molecular Biology.

are small, the deflection of the cantilever may be translated into applied force with Hooke's Law (*i.e.*, $F = -kx$, where F is force applied, k is an empirically determined spring constant, and x is deflection). This basic configuration, coupled with highly sensitive x–y position control, has been used for a wide array of applications including single molecule imaging and force spectroscopy.

The AFM has several characteristics that make it an attractive tool for examining fibrinogen adhesion to surfaces. In imaging mode, the AFM has resolution comparable to or better than electron microscopy, approaching sub-nanometre resolution in some cases.[4] A major advantage of the AFM over the electron microscope is the ability to perform experiments in either air or liquid, thus images and force data may be acquired for fully hydrated surfaces *in situ* as opposed to the vacuum necessary for electron microscopy.[5,6] Minimal surface preparation is necessary prior to imaging with the AFM, as the surface does not need to be conductive, fixed, or dyed. In addition, the compact size of the AFM allows it to be coupled with other methods such as surface plasmon resonance,[7] quartz crystal microbalance,[8] and optical microscopy.[9] As a force sensor, the AFM has a larger force range and superior spatial resolution than optical tweezers. As such, the AFM enables more straightforward study of protein adsorption strength, typically in the nano-Newton range.[10]

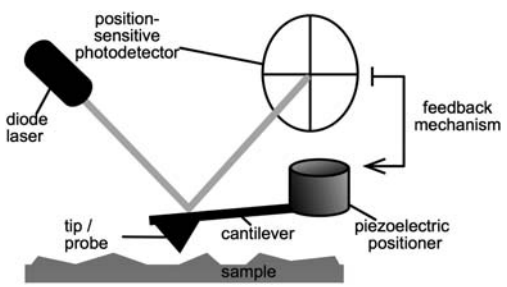

Fig. 2 General schematic of the atomic force microscope (AFM).

Due to its unique shape, relatively large size, and biological relevance, many research groups have employed fibrinogen to demonstrate the utility of AFM in studying protein adsorption.[5] Indeed, the first report of protein imaging in liquid investigated fibrin polymerization on mica,[11] and one of the first reported uses of non-contact AFM imaging to examine a biological sample was fibrinogen on silicon dioxide.[12] Since these seminal publications, fibrinogen has been used to demonstrate techniques for removing artifacts from single-molecule images,[13] filtering the abundance of data generated from force spectroscopy experiments,[14] and coupling the AFM to other instruments.[7,8]

Our goal with this review is to explore the methodology necessary to study fibrinogen using the AFM. Towards this goal, we separately address the imaging and force spectroscopy capabilities of the AFM. Methodological considerations are presented for each, while experimental motivations and associated parameters are discussed to identify best practices for data collection. Lastly, recent advances in applying the AFM's imaging and force spectroscopy modalities to studying fibrinogen are described. While we focus on fibrinogen due to its biological relevance and utility as a model biomacromolecule, the methods described herein may be easily applied to other proteins.

2. Imaging

Imaging of fibrinogen using AFM may be conducted in a number of ways including contact, alternating contact (*i.e.*, 'tapping'), and non-contact modes (Fig. 3).[6] Other AFM modes (*e.g.*, higher harmonic imaging) have not been used to characterize fibrinogen

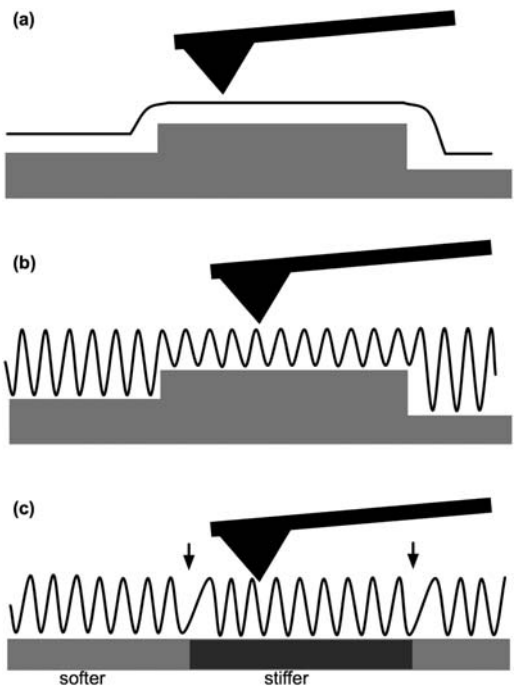

Fig. 3 Schematic of (a) contact and (b and c) intermittent contact or tapping mode imaging with the AFM. In tapping mode, (b) changes in topology are represented by changes in the amplitude of the oscillation, (c) while changes in sample stiffness are represented by changes in the oscillation's phase lag, indicated by arrows.

 This journal is © The Royal Society of Chemistry 2010

View Article Online

Published on 30 March 2010. Downloaded by Michigan State University on 19/01/2016 16:46:48.

adsorption. As such, these modes will not be discussed, but interested readers are directed to more general reviews on AFM of proteins.[15–18] In contact mode the tip is moved along the surface and topological changes in the substrate and/or difference in frictional force between the tip and substrate translate to deflections of the cantilever (Fig. 3a).[19] A feedback mechanism maintains the applied force between the tip and substrate by modulating the distance between the cantilever base and the substrate. Of note, this motion applies lateral force to the substrate capable of dislodging adhered objects.[20–24] In contrast, alternating contact or tapping mode is based on oscillating the tip near its resonance frequency as it is rastered along the surface. Changes in the amplitude and phase of the oscillations correspond to changes in the topology (Fig. 3b) and stiffness (Fig. 3c) of the sample, respectively. In turn, the latter enhances topographical images to provide molecular-scale resolution on rough surfaces.[25] Generally, little to no lateral forces to the substrate are observed *via* alternating contact mode, though the vertical forces may be large, altering the height of soft samples.[26] With respect to fibrinogen, Agnihotri and Siedlecki reported movement of surface-bound fibrinogen by the AFM probe in tapping mode,[27] suggesting the need for careful experimental design. Non-contact mode is similar to alternating contact mode in that the cantilever is oscillated near its resonance frequency and rastered across the surface. However, by reducing the amplitude and increasing the oscillation frequency, the probe responds to long-range attractive forces instead of short-range repulsive forces, as is the case for alternating contact mode.[15,26] While this mode of imaging provides high resolution with small impact forces, it is technically complex to execute and has therefore found limited use for imaging fibrinogen.[12,26]

2.1 Methodology

In addition to imaging mode, sample hydration and post-imaging analyses must be considered when imaging fibrinogen. While the ability to function in liquid sets the AFM apart from other microscopy techniques (*e.g.*, electron microscopy), imaging fully hydrated samples allows for a better representation of protein at the expense of imaging resolution. Gettens and Gilbert reported that fibrinogen molecules exhibit markedly different appearance in liquid than in air, including a reduction in volume of the adhered proteins in the dehydrated sample.[22] However, the superior resolution in air has allowed for the observation of fibrin features as small as αC domains.[20,28] Dehydrated proteins also adhere more strongly to surfaces than those in liquid, decreasing the likelihood that the AFM probe will disturb and distort the protein during imaging. While the appearance of the trinodular morphology of fibrinogen molecules imaged in air implies that the dehydrated protein retains much of its tertiary structure, caution must be exercised when interpreting the structural features identified in proteins imaged in air.

Sample preparation for protein imaging is highly dependent on the goals of the study. Imaging single molecules requires a low surface density of protein. As such, dilute solutions of protein (0.1–10 μg mL^{-1}) must be employed to prepare the substrate. In contrast, studies of bulk protein adsorption to biomaterials should use protein concentrations nearer to physiological conditions (2–3 mg mL^{-1},[29]). If the fibrinogen is to be imaged in air, the surface must be removed from the solution, rinsed, and dried in a manner that least disturbs the surface-bound protein, as contact with the air–water interface may denature adsorbed fibrinogen. Drying under a stream of nitrogen gas represents the most efficient and uniform method for drying a surface, as Ortega-Vinuesa *et al.* demonstrated that simply allowing a wet surface to dry under ambient conditions results in rings of denatured protein.[30] The time between surface modification and imaging also affects protein hydration and structure. For example, Ohta *et al.* reported protein spreading as a function of time following substrate preparation.[28] When imaging in liquid, it is possible to adsorb fibrinogen either *in situ* or *ex situ*. Immobilizing protein *in situ* with the aid of a flow cell device contributes minimal disturbances to the surface. Furthermore, real-time data may be acquired as images are collected throughout the process of protein immobilization.[19,21,22,25,27,31–35] However, flow cell accessories are often complicated to construct and use, and may be expensive. In addition, the physical interaction between the AFM probe and the protein during imaging may alter the kinetics of fibrinogen adsorption. Preparing surfaces *ex situ* enables the acquisition of 'snapshots' of the adsorption process without AFM probe interference.[21,22,34–36]

Both the size and shape of the AFM probe may result in imaging artifacts including lateral enlargement and false features.[6] When the object to be imaged and the probe (typical radius of ~5–10 nm) are of similar sizes, as is the case with fibrinogen (5 × 5 × 45 nm), the area of the object appears enlarged. The size and distinct trinodular shape of fibrinogen have made it an attractive model protein to test methods

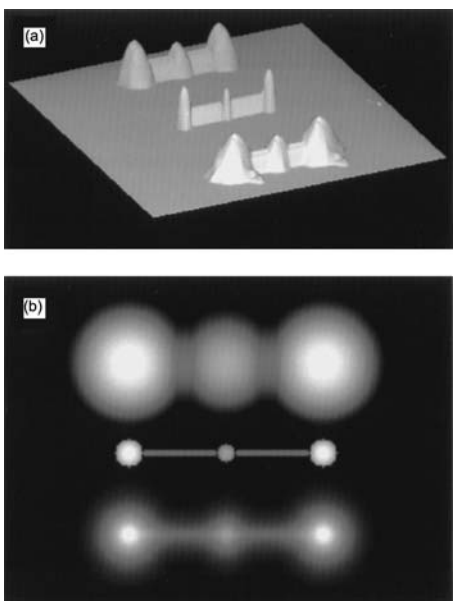

Fig. 4 (a) Model of fibrinogen molecule (center) imaged with defect-less probe (top) and defected (bottom) probes. (b) Model of fibrinogen (center) imaged with a wide probe (top) that is then eroded to restore the original size (bottom). Fibrinogen model consists of two large distal ellipsoids (diameter of 6.5 nm, height of 1.28 nm) and one central ellipsoid (diameter of 5 nm, height of 1 nm) linked by two cylinders (length of 14.75 nm, diameter of 1.2 nm) representing the D, E, and coiled-coil regions, respectively. Reproduced with permission from Wilson *et al.*[13] Copyright 1996, American Vacuum Society.

View Article Online

Published on 30 March 2010. Downloaded by Michigan State University on 19/01/2016 16:46:48.

designed to subtract probe shape artifacts from AFM images. In 1996, Wilson *et al.* introduced a method to restore the true shape of fibrinogen molecules imaged *via* AFM by first calibrating the tip size and shape with a sphere of known dimensions (Fig. 4).[13] Similar methodology was later applied to real images of fibrinogen by Marchant and co-workers.[31,32] While not yet the standard for fibrinogen imaging, Gettens and Gilbert acknowledged that their surface coverage-based adsorption kinetics studies would benefit from similar strategies.[22]

2.2 Single molecules to films of protein

When using the imaging mode of the AFM to study fibrinogen adsorption to a surface, the goals of a study dictate the amount of protein and imaging scale. The nanometre-scale resolution of the AFM on flat surfaces allows the size and morphology of single molecules to be analyzed for details regarding the interactions between the structures of fibrinogen and the substrate.[32,35,37–40] Alternatively, the height, roughness, and frictional forces of supra-monolayers of fibrinogen hold information about the amount and structure of the adsorbed protein.[19,41–44]

The mode of adhesion to different surfaces may be studied from the structure of single surface-bound fibrinogen molecules.[32,35,37–40] For example, Van De Keere *et al.* demonstrated that the different regions (*e.g.*, αC, D and E) mediate the protein's adhesion as a function of a substrate's surface properties, since the fibrinogen αC domains are positively charged and the D and E regions have a net negative charge with several external hydrophobic patches at neutral pH.[40] Marchin and Berrie reported on the importance of the αC domains promoting electrostatic attractions when fibrinogen adsorbs to negatively charged surfaces (*e.g.*, mica and titanium).[38] As such, the αC domains are impossible to resolve as they lie beneath the bulk of the molecule, and fibrinogen loses its trinodular morphology.[38] In contrast, the D and E regions facilitate adsorption to hydrophobic surfaces (*e.g.*, highly ordered pyrolytic graphite), leaving the αC domains to either remain associated with the E region or lay alongside the molecule. Toscano and Santore have resolved both fibrinogen's trinodular morphology and the αC domains next to or in contact with the E region on hydrophobic surfaces.[21]

Single molecule imaging has also been used to elucidate the structural stability of adsorbed fibrinogen on a specific substrate (*i.e.*, exposed to a specific surface chemistry).[20,27,28,32] Table 1 lists the sizes of single fibrinogen molecules with trinodular conformations found using the AFM. Proteins adsorbed to most surfaces undergo spreading to maximize surface area interacting with the substrate. Much of this spreading is associated with denaturing of the protein. Systematic studies exploiting the ability of the AFM to measure both the area and height of an object have examined the extent of fibrinogen spreading as a function of surface chemistry[20,32] and time.[27,28] Such measurements have proven highly dependent on the conditions under which the proteins were adsorbed and imaged (*i.e.*, whether in air or aqueous conditions, as a function of surface roughness, pH, and time of adsorption), making direct comparison difficult. Standardization of this field would be beneficial for future work.

The use of AFM to obtain information on the kinetics of fibrinogen adsorption further demonstrates the utility of imaging over more complex analytical methodology (*e.g.*, radiolabeling, fluorescence, surface plasmon resonance).[21,22,34,35] Such studies often require the scanning of larger areas (*e.g.*, 10 × 10 μm^2) to better quantify surface area coverage.[19,21,37,45] The resolution required for imaging protein monolayers is less than for discerning submolecular features on single fibrinogen molecules. To quantify fibrinogen adsorption to rough substrates, phase data from alternating-contact mode images can be used, since proteins such as fibrinogen have different mechanical properties than the underlying polymer, phase data effectively filters out any topological complexity of the substrate. Holland and Marchant resolved single fibrinogen molecules on rough polymer surfaces *via* phase imaging data.[25] In addition, Childs *et al.* used phase data to improve the resolution of fibrinogen adsorption to topologically complex polymer surfaces.[44] Alternatively, Milleding and co-workers evaluated the RMS values from the height data of images of fibrinogen films on ceramic-based dental implants as a measure of protein surface coverage.[41]

Table 1 Size of trinodular fibrinogen molecules found by AFM imaging

Substrate	Imaging conditions	Protein incubation[a]	Rinse	Length/nm	Width[b]/nm	Height[c]/nm	Study
Dichloro-dimethyl silane	Attractive force in air	4 h	Water	~60	—	<6	12
OTS	Tapping in liquid	1 h at 37 °C	Dilutions of PBS	48 ± 6	17 ± 6	1.3 ± 0.3	31
Mica coated with poly-L-lysine	Tapping in liquid	45 min	None	68 ± 1.2	—	3.9 ± 0.2	36
OTS	Tapping in liquid	1 h at 37 °C	Dilutions of PBS[d]	63.7 ± 7.0	14.3 ± 3.8	1.2 ± 0.3	32
APTES	Tapping in liquid	1 h at 37 °C	Dilutions of PBS[d]	55.7 ± 7.4	10.8 ± 2.3	1.9 ± 0.4	32
Mica	Tapping in liquid	1 h at 37 °C	Dilutions of PBS[d]	45.8 ± 4.3	10.3 ± 1.8	2.3 ± 0.4	32
Titanium	Tapping in liquid	1 h	Water	46 ± 3	—	1.4 ± 0.2	20
PMMA	Tapping in air	1 h	Water	48 ± 4	—	2.4 ± 0.4	54
HOPG	Tapping in air	10 min	Water	62 ± 9	28 ± 7	1.05 ± 0.13	38
HOPG	Tapping in liquid	10 min–2.5 h	PBS[d]	—	—	1.9–1[e]	27
Mica	Tapping in liquid	10 min–2.5 h	PBS[d]	—	—	1.2–2.1[e]	27
HOPG	Non-contact in air	5 min	Water	48	15	1.5	28
HOPG	Non-contact in air	1 day	Water	58	14–18	1.3	28
Polished glass	Tapping in liquid	Various	PBS[d]	~47	~10	~3	21
Oxidized silicon	Tapping in liquid	Various	PBS[d]	~47	~8	~2	21

[a] All surfaces incubated with protein at 25 °C unless otherwise noted. [b] Measured at widest point. [c] Measured at highest point. [d] Rinse was performed in flow-cell to minimize forces due to air–water interface. [e] Range of height values corresponds to respective range of incubation times.

 This journal is © The Royal Society of Chemistry 2010

View Article Online

Published on 30 March 2010. Downloaded by Michigan State University on 19/01/2016 16:46:48.

Other studies have sought to visualize the biological activity of surface-bound fibrinogen as it binds to thrombin,[33] liposomes,[46] or integrins,[47] or polymerizes to fibrin.[11,26,48–50] For example, Hussain *et al.* embedded nanogold-labeled integrins in a lipid-bilayer, using the labels to locate the integrins that were otherwise too small to resolve from the underlying substrate.[47] As expected due to the proximity of the C-terminus of the γ chains to the distal ends of the molecule, the fibrinogen was observed radiating outwards from the integrin-modified spheres. Abou-Saleh *et al.* reported varied polymerization of two types of fibrinogen, allowing connections between fibrin assembly and mechanical properties to be drawn.[26]

2.3 Surfaces

To understand what specific surface properties affect fibrinogen adsorption, AFM imaging has interrogated many substrate types. Studies have included high-resolution imaging of single molecules on ultraflat substrates like mica and highly oriented pyrolytic graphite (HOPG), and alkanethiol self-assembled monolayers (SAMs) to systematically alter surface chemistry. A universal requirement for such studies is homogeneity to foster uniform adsorption and minimize time scanning for areas of interest.

Historically, mica and HOPG have been employed to examine the morphology of single fibrinogen molecules with high resolution, due to their crystallinity, sub-nanometre root-mean-square (RMS) roughness, easy preparation, and affordability. In addition, the anionic and hydrophobic natures of mica and HOPG, respectively, allow one to probe the effect of principle chemical properties on fibrinogen adsorption. For example, Marchin and Berrie demonstrated that fibrinogen monomers assume different morphologies on the two surfaces, attributable to substrate hydrophobicity and charge.[38] Fibrinogen adsorbed to HOPG was characterized as having a clear trinodular structure, similar to that observed in prior TEM studies.[51,52] In contrast, fibrinogen adsorbed to mica was more globular in appearance, indicating a different mode of adsorption to the two surfaces. The authors hypothesized that the chemical properties of each region of fibrinogen dictated the mode of adsorption, and therefore final morphology of the protein. Since substrate preparation impacts the structure of the protein imaged, it is important to note that several groups have used the AFM to examine fibrinogen adsorption to both HOPG and mica at the single molecule level with varying results (Table 1).[27,28,32,38]

An important goal of early AFM studies was to explicitly examine the role of surface chemistry on protein adsorption to a surface. While specific substrates (*e.g.*, HOPG and mica) have been used to generate a desired surface chemistry, such surfaces are characterized by different surface topology and/or underlying chemical structure, making direct comparisons of fibrinogen adsorption challenging. To vary surface chemistry while maintaining the topographical and mechanical properties of the underlying substrate, researchers have used alkanethiol self-assembled monolayers (SAMs) on ultraflat gold substrates. Indeed, several groups have compared general fibrinogen adsorption to negatively charged and hydrophobic SAMs at the single molecule,[39] submonolayer,[43,45] and protein film[19] levels.

Due to its central role in evaluating the biocompatibility of a blood-contacting surface, much work has focused on examining fibrinogen adsorption to commonly employed and/or newly designed biomaterials. For example, fibrinogen adsorption has been evaluated on polystyrene,[53] polydimethylsiliconate (PDMS),[25,44] polymethylmethacrylate (PMMA),[54] and polyethyleneglycol (PEG)[42,55] polymers. Since the surface topography of most polymer films is rougher than HOPG and mica, polymeric substrates are more commonly used to assess bulk fibrinogen adsorption than single fibrinogen molecule adsorption. Fibrinogen adsorption to more traditional biomaterials such as titanium,[20,40] ceramics,[41] and stainless steel[22,34,35] has also been examined *via* AFM. Similar to the aforementioned polymers, the inherent topology of these materials generally limits their use to the study of protein films. However, methodologies have been developed to polish such surfaces to a degree suitable for single molecule imaging.[21,22,35,40]

Single experiments comparing the adsorption of fibrinogen to multiple surfaces are now possible using patterned substrates. Indeed, changes in frictional force,[19] height,[42] or phase[43] may be used to establish differences in the amount and conformation of fibrinogen adsorbed to different patterned regions on the substrate. Using patterned substrates, Ta and McDermott reported that the frictional forces observed at methyl- and carboxylate-terminated SAM regions evolved during fibrinogen adsorption.[19] They attributed such changes to protein denaturation, the rate of which differed depending on the surface chemistry.

2.4 Recent advances

While early work in AFM imaging of fibrinogen focused on obtaining high-resolution images of single molecules, extracting increasing amounts of information from larger groups of protein represents more recent advances. Toscano and Santore have used the AFM to observe the kinetics of fibrinogen adsorption to silica-based surfaces (*i.e.*, native oxide on silicon and acid-etched glass).[21] By counting individual molecules on surfaces exposed to fibrinogen solutions, they were able to detect fibrinogen adsorption at the transport-limited rate. They found that changes in fibrinogen adsorption were not measurable by the AFM after two minutes due to surface crowding. Since other tools (*e.g.*, total internal reflectance fluorescence) indicated that fibrinogen adsorption was diffusion limited (*i.e.*, minimal surface crowding) at these times, the method of counting fibrinogen molecules in AFM micrographs proved limited to protein coverage at which individual proteins were discernible. An alternative method was thus introduced by Gettens and Gilbert, whereby the kinetics of fibrinogen adsorption to biologically relevant materials was evaluated by AFM using model substrates including stainless steel, HOPG and mica.[22,34,35] Briefly, kinetic information was obtained by fitting the surface coverage of substrates immersed in fibrinogen solutions for different periods of time with a Langmuir curve. Due to tip effects artificially enlarging protein areas, this method overestimated the surface coverage, resulting in notable error.

Methodology for identifying specific proteins in heterogeneous films has recently been reported.[9,56] For example, researchers have modified AFM probes with anti-fibrinogen antibodies to

View Article Online

Published on 30 March 2010. Downloaded by Michigan State University on 19/01/2016 16:46:48.

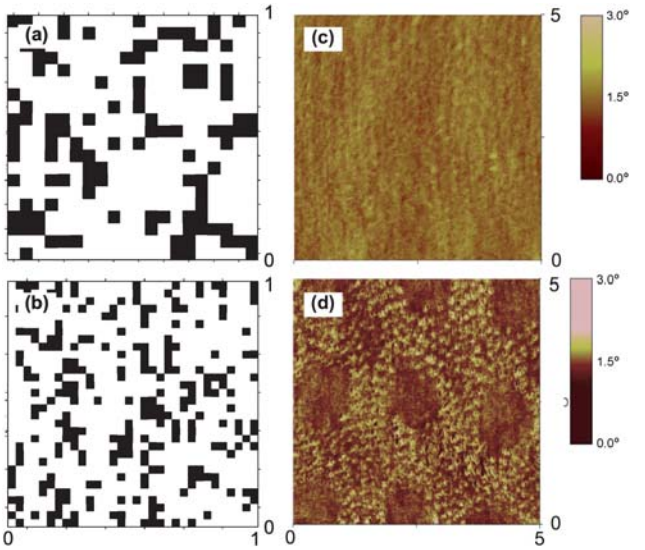

Fig. 5 Examples of molecular recognition with antibody-modified tips. All scales are in μm. (a, b) Force maps of fibrinogen covalently immobilized on a gold substrate using a probe modified with a monoclonal antibody recognizing the C-terminus of the fibrinogen γ chain with pixel resolutions of (a) 50 nm and (b) 32 nm. Black pixels represent force curves where interactions were observed (and therefore a fibrinogen molecule was present). (c, d) Tapping mode phase image of a mica surface patterned with bovine serum albumin and fibrinogen using (c) an unmodified probe and (d) a probe modified with a polyclonal fibrinogen antibody. The protein pattern may be discerned in (d), where the bovine serum albumin is in the light region and the fibrinogen is in the dark region. Force maps adapted with permission from Averett *et al.*[73] Copyright 2008, American Chemical Society. Phase images reprinted with permission from Soman *et al.*[58] Copyright 2008, Elsevier.

acquire either a map of force *versus* distance traces (*i.e.*, force curves),[57] or phase data images *via* tapping mode.[43] Although plagued by lower resolution, force mapping results in highly accurate location data regarding adsorbed fibrinogen (Fig. 5a and b). Similarly, analysis of alternating contact mode phase data for such experiments indicates where the attraction between the tip and substrate is strongest with improved lateral resolution and analysis time (Fig. 5c and d). A technique to detect fibrinogen molecules in heterogeneous protein films without modifying the AFM probe was demonstrated by Soman *et al.*, who used immunochemistry to label the substrate-bound protein with gold nanoparticles, objects of larger, more discernible size.[58]

3. Force spectroscopy

Whereas the imaging features of AFM allow for a detailed visual examination of adhered fibrinogen, the force mode enables the characterization of adhesion strength. In force-mode experiments, fibrinogen is nonspecifically adsorbed to the AFM probe prior to bringing the probe toward and away from a substrate of interest at a constant velocity. In this manner, adhesive forces between the probe and substrate are measured as deflections upon cantilever retraction (Fig. 6). The force of this deflection, deduced from Hooke's law, grows until it exceeds the adhesive force, at which time the bond between the tip and substrate breaks. By acquiring several hundred force curves, the average or

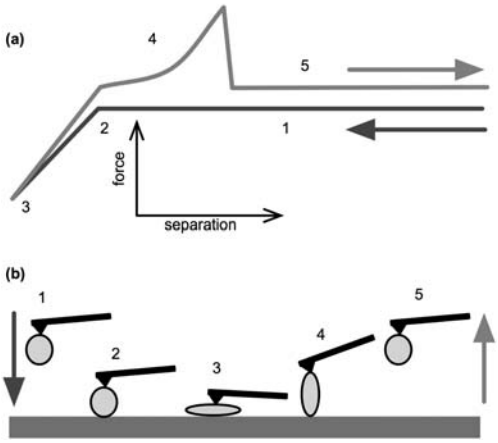

Fig. 6 (a) Idealized force curve and (b) corresponding motions of the AFM probe. The tip approaches the substrate (1) with zero deflection, (2) making contact and (3) pressing into the substrate to a pre-determined set point. If a bond exists between the tip and substrate, (4) the cantilever deflects as it retracts until (5) the restoring force of the cantilever exceeds the strength of the bond, which ruptures and the cantilever continues to retract.

most probable forces of rupture are determined. Qualitatively, the rupture forces of systems with varying parameters such as protein type, substrate chemistry, or contact duration have been compared to deduce trends. Quantitatively, data have been compiled and analyzed with one of the many models available to determine the kinetics of the interactions. Both qualitative and quantitative studies are introduced below.

3.1 Methodology

Several methodological details must be considered when employing AFM force spectroscopy to examine fibrinogen adsorption, including protein immobilization, data analysis, and appropriate controls. The most common method for immobilizing fibrinogen to the AFM probe is nonspecific adsorption. Although simple, nonspecific adsorption often results in denatured proteins due to the large number of hydrophobic interactions involved in adhesion. Furthermore, it is possible for the protein to become dislodged from the surface during the course of the experiments, resulting in undesirable artifacts. Researchers have thus used crosslinkers such as glutaraldehyde to covalently attach fibrinogen to silicon-nitride AFM tips[59] and glass cover slips (substrates).[10]

Data analysis is a critical element for AFM force spectroscopy studies. Since protein-related force data are generally complex (*i.e.*, characterized by multiple ruptures), it is important to decipher which events correspond to protein desorption, structural changes, and/or thermal noise. In 2001, Gergely *et al.* described an algorithm designed to automatically choose events for analysis with the goal of minimizing operator bias, using the interactions of fibrinogen adsorbing to glass for proof-of-concept.[14] The algorithm first determined the standard deviation of the baseline thermal noise, then identified specific force events as some multiple of that value. While this method accounts for changes in force due to thermal fluctuations, it is not capable of discerning the source of rupture events.

 This journal is © The Royal Society of Chemistry 2010

View Article Online

Published on 30 March 2010. Downloaded by Michigan State University on 19/01/2016 16:46:48.

Performing multiple controls is imperative to ensure that the interactions observed in force spectroscopy experiments are between the fibrinogen and surface of interest and reproducible. First, forces between the bare probe and the substrate should be investigated to assess the magnitude of background interactions. To minimize effects in the data attributable to differences in protein immobilization, it may be advantageous to use a single protein-modified tip for as many experiments as possible. However, since denaturation of the fibrinogen on the tip over time is likely, it is necessary to perform controls demonstrating that trends are surface-dependent and not a function of analysis time.

3.2 Surfaces

Force spectroscopy with the AFM is relatively insensitive to substrate topology (*i.e.*, roughness). In contrast, physical properties of the substrate including stiffness and surface energy are important. Soft substrates (*e.g.*, membranes of cells) make determination of where the tip contacts the substrate and spring constant calculation difficult, and should thus be avoided. Nevertheless, soft substrates may be used if the goal is to obtain qualitative rather than quantitative information.

To generate knowledge about the properties of a substrate that influence adhesion, fibrinogen adsorption to model substrates including glass,[10,14,60–62] SAM-modified gold,[63,64] polymers,[10,65,66] and mica[59] has been studied. For example, Kidoaki and Matsuda compared the adhesion force of albumin, IgG, and fibrinogen to model SAM substrates. They found that regardless of the substrate's surface chemistry (*i.e.*, SAM) fibrinogen adhered more strongly than either IgG or albumin.[63] Similarly, Sethuraman *et al.* probed the adhesion strength of seven proteins on eight model surfaces,[64] reporting a correlation between the adhesion force and both the secondary structure and molecular weight of the protein. More recently, Xu and Siedlecki reported a strong correlation between the force of fibrinogen adhesion and the hydrophobicity of polymer-based substrate, with a notable decrease in force as the water-contact angle increased above $\sim 60^{\circ}$.[66]

Since force spectroscopy has greater tolerance for nanometre-scale surface roughness than high-resolution AFM imaging, fibrinogen adsorption to a wider range of biologically relevant materials including dialysis membranes,[67] platelet membranes,[68] and dental implants[69] has been examined. Conti *et al.* found that nanometre-scale surface roughness (*i.e.*, RMS values ranging from 0.3 to 5 nm) correlated with the adhesion strength of fibrinogen on both hydrophobic and hydrophilic dialysis membranes.[67] This result was expected because greater surface roughness increased the surface area for protein–surface interactions. However, Xu and Siedlecki reported that surface roughness (*i.e.*, RMS values between 4 and 13 nm) was not a significant parameter in fibrinogen adsorption to surfaces.[66]

3.3 Parameters

To characterize fibrinogen adsorption with force spectroscopy, researchers have examined the force of adhesion as a function of loading rate (*i.e.*, how fast the force applied to the bond is increased with time) and dwell time (*i.e.*, the amount of time the tip is in contact with the substrate). Since bonds under force are not at equilibrium (*i.e.*, the lowest energy state), the loading rate affects the force required to rupture the bond.[70] While the nominal loading rate is a product of the spring constant of the AFM cantilever (measured in N m^{-1}) and the retraction velocity (measured in m s^{-1}), the tether between the tip and substrate may cause the loading rate to deviate from its nominal value. In such cases the slope of the force curve just prior to bond rupture may be used to determine the loading rate. Several models have been developed to extract the rupture kinetics of single bonds from the relationship between the force of rupture and the loading rate, the most common being the Bell–Evans model.[70,71] As the determinant of the contact time of the protein with the substrate, the dwell time mediates how many and what type of bonds (*e.g.*, electrostatic involving residues on the surface of fibrinogen, or hydrophobic involving buried residues normally at the protein core) develop between the proteins adhered to the probe and the substrate. Both loading rate and dwell time studies have enabled the elucidation of how fibrinogen adsorption is influenced by the dynamic environment created by blood flow in the circulatory system.[10,60–62,66,69]

In 2000, Gergely *et al.* used fibrinogen as an example protein to demonstrate the application of the Bell–Evans model to nonspecific protein adsorption.[61] The shortcoming of this study was an inability to distinguish the adsorption of single fibrinogen molecules, as multiple molecules were immobilized to each tip. The same research group later created a model for protein adsorption that accounted for multiple adhesion points between the probe and substrate, resulting in a better fit between fibrinogen adsorption and the Bell–Evans construct.[62]

A few research groups have investigated the dwell-time dependence of fibrinogen adsorption to glass,[60] dental implant surfaces (*i.e.*, calcium phosphate and titanium),[69] and colloidal glass and polymer probes.[10,66] Of note, each study found that the rupture force of fibrinogen adsorption increased with dwell time, maximizing after several seconds. These reports indicate that the conformational changes of fibrinogen responsible for adhesion are completed within seconds after the protein contacts a surface. Xu and Siedlecki reported that the saturation force was loading rate-dependent, signifying that the conformational changes responsible for fibrinogen adhesion followed kinetic trends similar to single bonds.[10]

3.4 Recent advances

A common drawback of force spectroscopy investigations of fibrinogen adsorption is the time- and force-dependent denaturation of the protein. Since the same small set of fibrinogen molecules immobilized on the AFM probe are used for potentially thousands of force measurements, conformational changes to the protein over the course of an experiment often introduce systematic artifacts in the data. Furthermore, the small number of proteins examined (*i.e.*, those immobilized on the probe) restricts investigation of the ensemble of fibrinogen molecules. To overcome these difficulties, Xu and Siedlecki immobilized a colloidal probe with the surface functionality of interest to the AFM cantilever, and adsorbed fibrinogen to the substrate.[10] Each force curve was acquired at a different location on the sample, ensuring that a new protein was examined with each

View Article Online

Published on 30 March 2010. Downloaded by Michigan State University on 19/01/2016 16:46:48.

measurement. This method eliminated force-dependent denaturation artifacts and increased the ensemble of fibrinogen molecules measured throughout the experiment. Using such methodology, the authors reported variation between the kinetics of fibrinogen adsorption to hydrophilic and hydrophobic substrates. At hydrophobic substrates, the relationship between the loading rate and rupture force of fibrinogen adsorption proved biphasic, indicating the existence of multiple energy barriers. The interactions between fibrinogen and hydrophilic surfaces exhibited a single energy barrier. It is important to note that more recently developed models of forced bond rupture, including the Dudko–Hummer model, predict curvature in the relationship between loading rate and force.[72] In this respect, it is possible that the non-linear nature of the interaction between fibrinogen and hydrophobic surfaces may be better explained by the Dudko–Hummer model than multiple energy barriers in the Bell–Evans model. Although the population of fibrinogen molecules probed was increased by adsorbing the fibrinogen to the substrate, examining fibrinogen adsorption at the single-molecule level remains elusive. Since force spectroscopy data are most reliably interpreted when they represent the rupture of single bonds, future experiments will benefit from improved methodology for examining single molecules.

The versatility of AFM has enabled the study of the mechanical nature of fibrinogen's polymerized form (*i.e.*, fibrin) by applying and monitoring forces to molecules and molecular assemblies. Using AFM, researchers have probed fibrin's mechanics from large fibers down to single molecules.[73–75] For example, Averett *et al.* examined specific interactions between fibrin monomers by immobilizing fibrinogen fragments and protein variants containing complementary binding sites on the AFM tip and substrate.[73,75] Perhaps not surprising based on earlier fiber and oligomer studies, the interaction responsible for fibrin polymerization was strong enough to withstand unfolding of the molecular structure. Forced rupture of this bond was often preceded by a series of abrupt changes in the length of fibrinogen, to a maximum of ~50% strain.

To date, the mechanics of two kinds of fibrin(ogen) oligomers have been examined with the AFM: chains of fibrinogen molecules linked covalently end-to-end,[76] and naturally occurring double-stranded half-staggered protofibrils.[77,78] In each case, the oligomer was noncovalently adsorbed to the surface at a low density, and force curves were acquired with bare AFM probes. When extended, periodicity in the force curve was attributed to unfolding of sequential domains (*i.e.*, fibrin(ogen) coiled coils). Currently, some disagreement exists on whether the extension of the coiled-coil should occur as a plateau of constant force as each hydrogen bond is broken (*i.e.*, unzipped),[77] or a sawtooth pattern with maximum force followed by entropic extension of disordered protein.[76,78] Future AFM studies will undoubtedly address this quandary.

4. Conclusions

Since the inception of the atomic force microscope, the examination of protein adsorption to surfaces at the molecular level has evolved into a dynamic field of study. Fibrinogen has served as a model protein for both the imaging and force modes of the AFM due to its unique size, shape, and biological relevance. Indeed, many fundamental AFM methodologies related to studying protein adsorption including liquid imaging,[11] image analysis,[13] and adsorption kinetics[35] have been validated using fibrinogen. Since these seminal works, similar methodologies have been used to investigate the adsorption of other proteins such as immunoglobulin G,[79,80] albumin,[81] and spider silk[82] to surfaces. Furthermore, AFM has enabled an improved understanding of fibrinogen biochemistry at interfaces. The rate of continuing advances in AFM methodology and data analyses indicate that it will remain a viable tool for probing biological systems and phenomena.

Acknowledgements

The authors gratefully acknowledge the National Science Foundation (CHE-0349091) for support of their AFM-related research.

References

1 C. J. Wilson, R. E. Clegg, D. I. Leavesley and M. J. Pearcy, *Tissue Eng.*, 2005, **11**, 1–18.
2 S. T. Lord, *Curr. Opin. Hematol.*, 2007, **14**, 236–241.
3 G. Binnig, C. Quate and C. Gerber, *Phys. Rev. Lett.*, 1986, **56**, 930–933.
4 Y. Dufrêne, *Nat. Rev. Microbiol.*, 2008, **6**, 674–680.
5 R. E. Marchant, I. Kang, P. S. Sit, Y. Zhou, B. Todd, S. J. Eppell and I. Lee, *Curr. Protein Pept. Sci.*, 2002, **3**, 249–274.
6 Y. F. Dufrene, *Nat. Protocols*, 2008, **3**, 1132–1138.
7 X. Chen, M. C. Davies, C. J. Roberts, K. M. Shakesheff, S. J. B. Tendler and P. M. Williams, *Anal. Chem.*, 1996, **68**, 1451–1455.
8 K. Choi, J. Friedt, F. Frederix, A. Campitelli and G. Borghs, *Appl. Phys. Lett.*, 2002, **81**, 1335–1337.
9 Y. F. Dufrene and P. Hinterdorfer, *Eur. J. Phys.*, 2008, **256**, 237–245.
10 L. Xu and C. A. Siedlecki, *Langmuir*, 2009, **25**, 3675–3681.
11 B. Drake, C. Prater, A. Weisenhorn, S. Gould, T. Albrecht, C. Quate, D. Cannell, H. G. Hansma and P. Hansma, *Science*, 1989, **243**, 1586–1589.
12 R. Wigren, H. Elwing, R. Erlandsson, S. Welin and I. Lundstrom, *FEBS Lett.*, 1991, **280**, 225–228.
13 D. L. Wilson, P. Dalal, K. S. Kump, W. Benard, P. Xue, R. E. Marchant and S. J. Eppell, *J. Vac. Sci. Technol., B*, 1996, **14**, 2407–2416.
14 C. Gergely, B. Senger, J. C. Voegel, J. K. Horber, P. Schaaf and J. Hemmerle, *Ultramicroscopy*, 2001, **87**, 67–78.
15 R. Garcia and R. Perez, *Surf. Sci. Rep.*, 2002, **47**, 197–301.
16 N. Jalili and K. Laxminarayana, *Mechatronics*, 2004, **14**, 907–945.
17 J. Preiner, J. Tang, V. Pastushenko and P. Hinterdorfer, *Phys. Rev. Lett.*, 2007, **99**, 046102.
18 P. L. Frederix, P. D. Bosshart and A. Engel, *Biophys. J.*, 2009, **96**, 329–338.
19 T. C. Ta and M. T. McDermott, *Anal. Chem.*, 2000, **72**, 2627–2634.
20 P. Cacciafesta, A. D. L. Humphris, K. D. Jandt and M. J. Miles, *Langmuir*, 2000, **16**, 8167–8175.
21 A. Toscano and M. M. Santore, *Langmuir*, 2006, **22**, 2588–2597.
22 R. T. Gettens and J. Gilbert, *J. Biomed. Mater. Res., Part A*, 2007, **81**, 465–473.
23 S. M. Deupree and M. H. Schoenfisch, *Langmuir*, 2008, **24**, 4700–4707.
24 B. B. Lim, K. L. Venkatachalam, A. Jahangir, S. B. Johnson and S. J. Asirvatham, *J. Cardiovasc. Electrophysiol.*, 2008, **19**, 843–850.
25 N. Holland and R. E. Marchant, *J. Biomed. Mater. Res.*, 2000, **51**, 307–314.
26 R. H. Abou-Saleh, S. D. Connell, R. Harrand, R. A. Ajjan, M. W. Mosesson, D. A. M. Smith, P. J. Grant and R. A. Ariens, *Biophys. J.*, 2009, **96**, 2415–2427.
27 A. Agnihotri and C. A. Siedlecki, *Langmuir*, 2004, **20**, 8846–8852.

 This journal is © The Royal Society of Chemistry 2010

View Article Online

Published on 30 March 2010. Downloaded by Michigan State University on 19/01/2016 16:46:48.

28 R. Ohta, N. Saito, T. Ishizaki and O. Takai, *Surf. Sci.*, 2006, **600**, 1674–1678.
29 T. W. Meade, R. Chakrabarti, A. P. Haines, W. R. North and Y. Stirling, *Br. Med. J.*, 1979, **1**, 153–156.
30 J. L. Ortega-Vinuesa, P. Tengvall and I. Lundstrom, *J. Colloid Interface Sci.*, 1998, **207**, 228–239.
31 R. E. Marchant, M. D. Barb, J. R. Shainoff, S. J. Eppell, D. L. Wilson and C. A. Siedlecki, *Thromb. Haemostasis*, 1997, **77**, 1048–1051.
32 P. S. Sit and R. E. Marchant, *Thromb. Haemostasis*, 1999, **82**, 1053–1060.
33 P. S. Sit and R. E. Marchant, *Surf. Sci.*, 2001, **491**, 421–432.
34 R. T. Gettens, Z. Bai and J. Gilbert, *J. Biomed. Mater. Res., Part A*, 2005, **72**, 246–257.
35 R. T. Gettens and J. Gilbert, *J. Biomed. Mater. Res., Part A*, 2008, **85**, 176–187.
36 D. J. Taatjes, A. S. Quinn, R. J. Jenny, P. Hale, E. G. Bovill and J. McDonagh, *Cell Biol. Int.*, 1997, **21**, 715–726.
37 T. C. Ta, M. T. Sykes and M. T. McDermott, *Langmuir*, 1998, **14**, 2435–2443.
38 K. Marchin and C. Berrie, *Langmuir*, 2003, **19**, 9883–9888.
39 Y. Lin, J. Wang, L. J. Wan and X. H. Fang, *Ultramicroscopy*, 2005, **105**, 129–136.
40 I. Van De Keere, R. Willaert, A. Hubin and J. Vereecken, *Langmuir*, 2008, **24**, 1844–1852.
41 P. Milleding, A. Carlen, A. Wennerberg and S. Karlsson, *Biomaterials*, 2001, **22**, 2545–2555.
42 C. M. Yam, J. Gu, S. Li and C. Cai, *J. Colloid Interface Sci.*, 2005, **285**, 711–718.
43 E. Servoli, D. Maniglio, M. Aguilar, A. Motta, J. San Roman, L. Belfiore and C. Migliaresi, *Macromol. Biosci.*, 2008, **8**, 1126–1134.
44 M. Childs, D. Matlock, J. Dorgan and T. Ohno, *Biomacromolecules*, 2001, **2**, 526–537.
45 K. Marchin, S. Phung and C. Berrie, *e–J. Surf. Sci. Nanotechnol.*, 2005, **3**, 173–178.
46 E. Casals, A. Verdaguer, R. Tonda, A. Galan, G. Escolar and J. Estelrich, *Bioconjugate Chem.*, 2003, **14**, 593–600.
47 M. Hussain, A. Agnihotri and C. A. Siedlecki, *Langmuir*, 2005, **21**, 6979–6986.
48 K. M. Evans-Nguyen, R. R. Fuierer, B. D. Fitchett, L. R. Tolles, J. C. Conboy and M. H. Schoenfisch, *Langmuir*, 2006, **22**, 5115–5121.
49 H. Jung, J. Kim, Y. Kim, G. Tae, Y. Kim and D. Johannsmann, *Langmuir*, 2009, **25**, 7032–7041.
50 H. Jung, G. Tae, Y. Kim and D. Johannsmann, *Colloids Surf., B*, 2009, **68**, 111–119.
51 C. Hall, *Proc. Natl. Acad. Sci. U. S. A.*, 1956, **42**, 801–806.
52 C. Hall and H. Slayter, *J. Cell Biol.*, 1959, **5**, 11–16.
53 R. J. Green, J. Davies, M. C. Davies, C. J. Roberts and S. J. B. Tendler, *Biomaterials*, 1997, **18**, 405–413.
54 K. D. Jandt, *Surf. Sci.*, 2001, **491**, 303–332.
55 S. Sharma, R. W. Johnson and T. A. Desai, *Biosens. Bioelectron.*, 2004, **20**, 227–239.
56 P. Hinterdorfer and Y. F. Dufrene, *Nat. Methods*, 2006, **3**, 347–355.
57 A. Agnihotri and C. A. Siedlecki, *Ultramicroscopy*, 2005, **102**, 257–268.
58 P. Soman, Z. Rice and C. A. Siedlecki, *Micron*, 2008, **39**, 832–842.
59 P. Soman, Z. Rice and C. A. Siedlecki, *Langmuir*, 2008, **24**, 8801–8806.
60 J. Hemmerle, S. Altmann, M. Maaloum, J. K. Horber, L. Heinrich, J. C. Voegel and P. Schaaf, *Proc. Natl. Acad. Sci. U. S. A.*, 1999, **96**, 6705–6710.
61 C. Gergely, J. C. Voegel, P. Schaaf, B. Senger, M. Maaloum, J. K. Horber and J. Hemmerle, *Proc. Natl. Acad. Sci. U. S. A.*, 2000, **97**, 10802–10807.
62 C. Gergely, J. Hemmerle, P. Schaaf, J. K. Horber, J. C. Voegel and B. Senger, *Biophys. J.*, 2002, **83**, 706–722.
63 S. Kidoaki and T. Matsuda, *Langmuir*, 1999, **15**, 7639–7646.
64 A. Sethuraman, M. Han, R. S. Kane and G. Belfort, *Langmuir*, 2004, **20**, 7779–7788.
65 K. E. Bremmell, P. Kingshott, Z. Ademovic, B. Winther-jensen and H. J. Griesser, *Langmuir*, 2006, **22**, 313–318.
66 L.-C. Xu and C. A. Siedlecki, *Biomaterials*, 2007, **28**, 3273–3283.
67 M. Conti, G. Donati, G. Cianciolo, S. Stefoni and B. Samori, *J. Biomed. Mater. Res.*, 2002, **61**, 370–379.
68 I. Lee and R. E. Marchant, *Ultramicroscopy*, 2003, **97**, 341–352.
69 A. Boukari, G. Francius and J. Hemmerle, *J. Biomed. Mater. Res., Part A*, 2006, **78**, 466–472.
70 E. A. Evans and K. Ritchie, *Biophys. J.*, 1997, **72**, 1541–1555.
71 O. K. Dudko, J. Mathé, A. Szabo, A. Meller and G. Hummer, *Biophys. J.*, 2007, **92**, 4188–4195.
72 O. K. Dudko, G. Hummer and A. Szabo, *Phys. Rev. Lett.*, 2006, **96**, 108101.
73 L. E. Averett, C. B. Geer, R. R. Fuierer, B. B. Akhremitchev, O. V. Gorkun and M. H. Schoenfisch, *Langmuir*, 2008, **24**, 4979–4988.
74 L. A. Chtcheglova, G. T. Shubeita, S. K. Sekatskii and G. Dietler, *Biophys. J.*, 2008, **86**, 1177–1184.
75 L. E. Averett, M. H. Schoenfisch, B. B. Akhremitchev and O. V. Gorkun, *Biophys. J.*, 2009, **97**, 2820–2828.
76 A. E. X. Brown, R. I. Litvinov, D. E. Discher and J. W. Weisel, *Biophys. J.*, 2006, **92**, L39–L41.
77 B. B. Lim, E. H. Lee, M. Sotomayor and K. Schulten, *Structure*, 2008, **16**, 449–459.
78 A. E. X. Brown, R. I. Litvinov, D. E. Discher, P. K. Purohit and J. W. Weisel, *Science*, 2009, **325**, 741–744.
79 D. Cullen and C. R. Lowe, *J. Colloid Interface Sci.*, 1994, **166**, 102–108.
80 H. X. You and C. R. Lowe, *J. Colloid Interface Sci.*, 1996, **182**, 586–601.
81 M. M. Browne, G. V. Lubarsky, M. R. Davidson and R. H. Bradley, *Surf. Sci.*, 2004, **533**, 155–167.
82 T. Pirzer, M. Geisler, T. Scheibel and T. Hugel, *Phys. Biol.*, 2009, **6**, 025004.
83 Y. I. Veklich, O. V. Gorkun, L. V. Medved, W. Nieuwenhuizen and J. W. Weisel, *J. Biol. Chem.*, 1993, **268**, 13577–13585.